Formally Exact Truncated Nonuniform Excess Helmholtz Free Energy Density Functional: Test and Application

Shiqi Zhou*

Research Institute of Modern Statistical Mechanics, Zhuzhou Institute of Technology, Wenhua Road, Zhuzhou City, 412008, P. R. China

Received: September 3, 2003; In Final Form: December 27, 2003

The functional expansion of the nonuniform excess Helmholtz free energy density functional around the bulk density was truncated at the first order, and then the functional counterpart of the Lagrangian theorem of differential calculus was employed to make the truncation formally exact. The concrete procedure is the following: According to the Lagrangian theorem and the definition of the direct correlation function (DCF), the original expansion coefficient, ,that is, the uniform first-order DCF, was replaced by the nonuniform first-order DCF whose density argument is an appropriate mixture of the density distribution and the bulk density with an adjustable parameter. With reference to the weighted density approximation, the nonuniform first-order DCF was then approximated by its uniform counterpart with a weighted density as its density argument. The weighting function was specified by equating the second-order functional derivative of the present truncated nonuniform excess Helmholtz free energy density functional with respect to the density distribution in the uniform limit to the second-order bulk DCF; the normalization condition of the weighting function specifies the adjustable parameter to be 0.5. The truncated expansion was incorporated into the density functional theory (DFT) formalism to predict the nonuniform hard-sphere fluid density distribution in good agreement with simulation data for three confining geometries: a single hard wall, a spherical cavity, and a bulk hard-sphere particle. The nonuniform Lennard-Jones fluid was investigated by dividing the bulk second-order DCF into a strongly density-depending short-range part and a weakly density-depending long-range part. The latter is treated by functional perturbation expansion truncated at the lowest order whose accuracy depends on how weakly the long-range part depends on the bulk density. The former is treated by the present truncated approximation. The two approximations are put into the density profile equation of the DFT to predict the density distribution for the Lennard-Jones fluid under the influence of two external potentials. The predicted density distribution displays even higher accuracy than that of two previous density functional perturbation theories in the region away from the repulsive wall but is a little inferior to the former approaches in the region near the wall. Also, a functional integral procedure was employed to develop the density functional approximation for the nonuniform first-order DCF to calculate the global thermodynamic properties of the nonuniform fluid.

I. Introduction

The statistical mechanical description of surface phenomena has become an active field in the past decade. One of focuses is the prediction of the single-particle density distribution. One of the available methods is that starting from the so-called Ornstein−Zernike equation and the other is that starting from a density functional expression, that is, the free energy density functional or the first-order direct correlation function density functional. The latter method is known as the so-called density functional theory. Several types of density functional approximations are proposed,[1] known as the functional perturbation expansion approximation, the weighted density approximation, the fundamental measure functional, and the density functional approximation based on the universality principle and test particle trick. The density functional approach has become a universal tool for the study of surface phenomena, such as the solid−liquid interface, solid−liquid phase transition, nucleation, wetting, liquid crystals, polymer statistical mechanics, and so on.

Recently, a density functional approximation for the nonuniform first-order direct correlation function (DCF) $C^{(1)}(\mathbf{r};[\rho])$ was proposed by the present author;[2] in this density functional approximation $C^{(1)}(\mathbf{r};[\rho])$ was expanded around the bulk density, then the series was truncated at the lowest order, and the functional counterpart of the Lagrangian theorem of differential calculus was employed to make the truncation formally exact. The density functional approximation was employed for the study of several interaction potential fluids, and good prediction accuracy was achieved. However, an adjustable parameter λ has to be incorporated into the density functional approximation, which makes the application of the density functional approximation very inconvenient. So, it will be very valuable if the adjustable parameter λ can be deleted from the density functional formalism. We note that the density functional approximation in ref 2 is obtained by expanding the $C^{(1)}(\mathbf{r};[\rho])$ around the bulk density; in fact, the same procedure also can be employed to expand the nonuniform excess Helmholtz free energy density functional $F_{ex}[\rho]$ around the bulk density. Following this idea, we find that the resulting density functional approximation for $C^{(1)}(\mathbf{r};[\rho])$ can be free of any adjustable

* Corresponding author. E-mail: chixiayzsq@yahoo.com.

10.1021/jp0366318 CCC: $27.50
Published on Web 02/10/2004

parameter. On the other hand, the nonhard-sphere interaction potential fluids are usually treated[3] by dividing the interaction potential into a short-range, repulsive part and a smoothly varying, long-range, attractive tail and then treating the former with the density functional approximation for a hard-sphere model fluid and the latter by thermodynamic perturbation theory or mean field approximation. However, we think that the correlation functions are related with the interaction potential nonlinearly, and the former is a functional of the latter. By solving the Ornstein−Zernike integral equation, all of the nonlinearity is integrated into the correlation functions, so it is more reasonable to divide the correlation functions rather than the interaction potential itself. In recent years some density functional approximations for the $C^{(1)}(\mathbf{r};[\rho])$ were proposed; all of them are exclusively employed for calculation of the density distribution profile. In fact, it is necessary sometimes to calculate the system free energy for some cases, which include phase behaviors under confined conditions, the calculation of surface tension, wetting transitions, and so forth.[1] Obviously, developing the density functional approximations for the $C^{(1)}(\mathbf{r};[\rho])$ to be employed for calculation of global thermodynamic properties will be very valuable. In Section II we will propose the present density functional approximation for $F_{ex}[\rho]$ and $C^{(1)}(\mathbf{r};[\rho])$. To test the present approximation, we will apply it to the hard-sphere model fluid under the influence of several external potentials and calculate the surface tension of a hard-wall−hard-sphere interface as a function of the bulk hard-sphere fluid density in Section III. We will also combine the present approximation with the partitioning procedure based on the bulk second-order DCF to calculate the density distribution profile for a nonuniform Lennard-Jones (LJ) fluid in Section III. Finally, in Section IV some conclusions are summarized.

II. Formulation of the New Density Functional Approximation Free of Adjustable Parameters

A formal "Taylor series" expansion of the nonuniform excess Helmholtz free energy density functional $F_{ex}[\rho]$ around a uniform system of bulk density ρ_b can be always written

$$F_{ex}[\rho] = F_{ex}(\rho_b) - \int C_0^{(1)}(\rho_b)[\rho(\mathbf{r}) - \rho_b]\, d\mathbf{r} - \sum_{n=3}^{\infty}\frac{1}{(n-1)!}\int d\mathbf{r}_1 \int d\mathbf{r}_2 \cdots \int d\mathbf{r}_{n-1} \prod_{m=1}^{n-1}[\rho(\mathbf{r}_m) - \rho_b] C_0^{(n-1)}(\mathbf{r}_1, \cdots, \mathbf{r}_{n-1};\rho_b) \quad (1)$$

Here, each functional derivative, that is, the expansion coefficient $C_0^{(n-1)}(\mathbf{r}_1,\mathbf{r}_2,\cdots,\mathbf{r}_{n-1};\rho_b)$ $n \geq 2$, is evaluated at the initial ρ_b. When such a series is terminated, it can be made an accurate representation by having the last functional derivative evaluated not at the initial ρ_b but at some $\rho_b + \lambda(\rho - \rho_b)$, with λ between 0 and 1;[4] this is actually a functional counterpart of the well-known Lagrangian theorem of differential calculus which states that the following eq 2 is exact if the value of λ is correctly chosen. According to the above procedure, we truncated the series at the first order; then eq 1 reduces to

$$F_{ex}[\rho] = F_{ex}(\rho_b) - \int C^{(1)}(\mathbf{r};[\rho_b + \lambda(\rho - \rho_b)])[\rho(\mathbf{r}) - \rho_b]\, d\mathbf{r} \quad (2)$$

In the above equation, subscript 0 stands for the uniform case and its absence corresponds to the nonuniform case. It should be noted that the expansion coefficient $C_0^{(1)}$ in eq 1 was replaced by $C^{(1)}$ in eq 2 because of substitution of the bulk density ρ_b by the nonuniform density field $\rho_b + \lambda(\rho - \rho_b)$; this replacement has to be done to be in agreement with the definition of the DCF. Equation 2 is exact and it does not include any approximation.

The key is to approximate the nonuniform first-order DCF $C^{(1)}(\mathbf{r};[\rho_b + \lambda(\rho - \rho_b)])$ and choose the appropriate mixing parameter λ. Following the spirit of the weighted density approximation,[5] it is reasonable for one to specify the former as

$$C^{(1)}(\mathbf{r};[\rho_b + \lambda(\rho - \rho_b)]) = C_0^{(1)}(\tilde{\rho}(\mathbf{r},\lambda)) \quad (3)$$

where the weighted density $\tilde{\rho}(\mathbf{r},\lambda)$ is defined as usual

$$\tilde{\rho}(\mathbf{r},\lambda) = \int d\mathbf{r}'\, w(|\mathbf{r} - \mathbf{r}'|;\rho_b)[\rho_b + \lambda(\rho(\mathbf{r}') - \rho_b)] \quad (4)$$

Here, to simplify the calculation, the density argument of the weighting function w is chosen as the bulk density ρ_b following the spirit of the simple weighted density approximation.[6]

To determine the weighting function w and mixing parameter λ, we carry out the functional derivative of eq 2 with respect to the density distribution $\rho(\mathbf{r})$ according to following formula:

$$C^{(2)}(\mathbf{r},\mathbf{r}';[\rho]) = \frac{-\beta\delta^2 F_{ex}[\rho]}{\delta\rho(\mathbf{r})\,\delta\rho(\mathbf{r}')} \quad (5)$$

In the limit of uniform density $\rho(\mathbf{r}) \rightarrow \rho_b$, the left side of eq 5 becomes $C_0^{(2)}(|\mathbf{r} - \mathbf{r}'|;\rho_b)$. Combination of eqs 2−5 with the uniform density limit taken after the functional derivatives leads to

$$w(|\mathbf{r} - \mathbf{r}'|;\rho_b) = \frac{C_0^{(2)}(|\mathbf{r} - \mathbf{r}'|;\rho_b)}{2\lambda C_0^{(1)'}(\rho_b)} \quad (6)$$

The normalization condition of the weighting function w specifies the value of λ to be 0.5 since $C_0^{(1)'}(\rho_b) = \int d\mathbf{r}\, C_0^{(2)}(\mathbf{r};\rho_b)$.

A new $C^{(1)}(\mathbf{r};[\rho])$ different from eq 3 can be obtained by carrying out the first-order derivative functional of eq 2 with respect to the density distribution $\rho(\mathbf{r})$

$$C^{(1)}(\mathbf{r};[\rho]) = C_0^{(1)}(\tilde{\rho}(\mathbf{r},\lambda)) + \int C_0^{(1)'}(\tilde{\rho}(\mathbf{r}',\lambda))\lambda w(|\mathbf{r} - \mathbf{r}'|;\rho_b)[\rho(\mathbf{r}') - \rho_b]\, d\mathbf{r}' \quad (7)$$

Equation 7 is the main result of the present contribution; combining eq 7 with the density profile equation eq 8 gives

$$\rho(\mathbf{r}) = \rho_b \exp\{-\beta\varphi_{ext}(\mathbf{r}) + C^{(1)}(\mathbf{r};[\rho]) - C_0^{(1)}(\rho_b)\} \quad (8)$$

Here, $\varphi_{ext}(\mathbf{r})$ is the external potential responsible for generation of the density distribution $\rho(\mathbf{r})$ and $\beta = 1/kT$ with k the Boltzmann constant and T the absolute temperature; one can obtain the operational equation for calculation of the density distribution.

$$\rho(\mathbf{r}) = \rho_b \exp\{-\beta\varphi_{ext}(\mathbf{r}) + C_0^{(1)}(\tilde{\rho}(\mathbf{r},\lambda)) + \int C_0^{(1)'}(\tilde{\rho}(\mathbf{r}',\lambda))\lambda w(|\mathbf{r} - \mathbf{r}'|;\rho_b)[\rho(\mathbf{r}') - \rho_b]\, d\mathbf{r}' - C_0^{(1)}(\rho_b)\} \quad (9)$$

It should be noted that by functional integration of $C^{(1)}(\mathbf{r};[\rho]) = (-\beta\delta F_{ex}[\rho])/\delta\rho(\mathbf{r})$ with the integration path chosen as $\rho_\alpha(\mathbf{r})$

$= \rho_b + \alpha(\rho(\mathbf{r}) - \rho_b)$, an expression for $\beta F_{ex}[\rho]$ similar to eq 2 can be obtained.

$$\beta F_{ex}[\rho] = \beta F_{ex}(\rho_b) - \int_0^1 d\alpha \int C^{(1)}(\mathbf{r};[\rho_b + \lambda(\rho - \rho_b)])[\rho(\mathbf{r}) - \rho_b]\, d\mathbf{r} \quad (2')$$

The difference between eq 2 and eq 2′ lies in that in the former a residual parameter appears in the argument of the direct correlation function, whereas in the latter there is not any residual parameter appearing in the final expression due to an integral over the path parameter. The difference originates from the different derivation path; one is based on the truncated Taylor series combined with the Lagrangian theorem, whereas the other is based on the functional integration. In the present presentation, the residual parameter is specified as a constant by the normalization condition of the weighting function whose density argument is taken to be the bulk density. However, even if the density argument is chosen as the weighted density as in the coupled weighted density approximation, the final result does not change.

III. Test and Application of the Present Density Functional Approximation

One regular method for testing a density functional approximation is to employ it for a nonuniform hard-sphere model fluid. We will test several cases: external potential, a single hard wall, a spherical cavity, and an external field due to a test hard-sphere particle chosen from a bulk hard-sphere fluid. In the case of a single hard wall, we also will calculate the surface tension of a hard-wall−hard-sphere interface.

The external potential for the above cases is of the following form, respectively

$$\varphi_{ext}(z) = \infty \quad z/\sigma < 0$$
$$= 0 \quad 0 < z/\sigma \quad \text{for a single hard wall} \quad (10)$$

$$\varphi_{ext}(\mathbf{r}) = \infty \quad |\mathbf{r}|/\sigma > R$$
$$= 0 \quad |\mathbf{r}|/\sigma < R \quad \text{for a spherical cavity} \quad (11)$$

$$\varphi_{ext}(\mathbf{r}) = \infty \quad |\mathbf{r}|/\sigma < 1$$
$$= 0 \quad |\mathbf{r}|/\sigma > 1 \quad \text{for a bulk hard-sphere particle} \quad (12)$$

In the case of a bulk hard-sphere particle, by use of the test particle trick by Percus,[7] the nonuniform density distribution $\rho(\mathbf{r})$ is related to the radial distribution function $g(\mathbf{r})$ of the bulk fluid by the following relation:

$$\rho(\mathbf{r}) = \rho_b g(\mathbf{r}) \quad (13)$$

The needed quantity, that is, the uniform second-order DCF, is from the Percus−Yevick approximation.[8] The calculated density distribution was plotted against the corresponding simulation data[9] in Figures 1 and 2 for the case of a single hard wall, in Figure 3 for the case of a spherical cavity, and in Figure 4 for the case of a bulk hard-sphere particle. From Figures 1 and 2 one can see that the present approximation is even comparable to the previous coupled weighted density approximation in accuracy.[10]

To calculate the system free energy from the present density functional approximation, we employ the functional integration method.

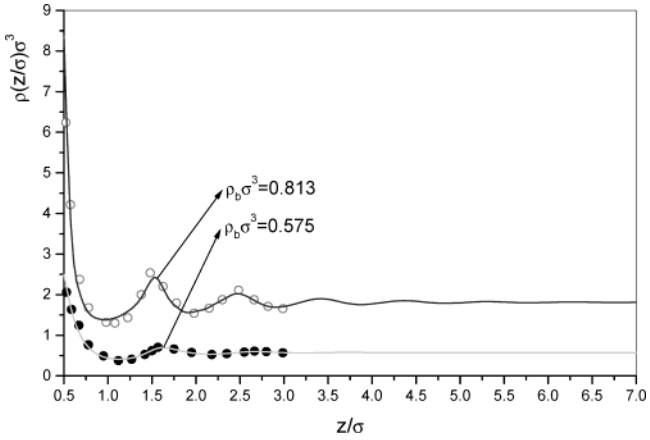

Figure 1. Density profiles of a hard-sphere fluid near a hard wall for two bulk densities $\rho_b\sigma^3 = 0.575$ and $\rho_b\sigma^3 = 0.813$, respectively. The ordinate for the curve above should be shifted down 1 unit. Lines stand for present prediction; symbols for simulation data.[9a]

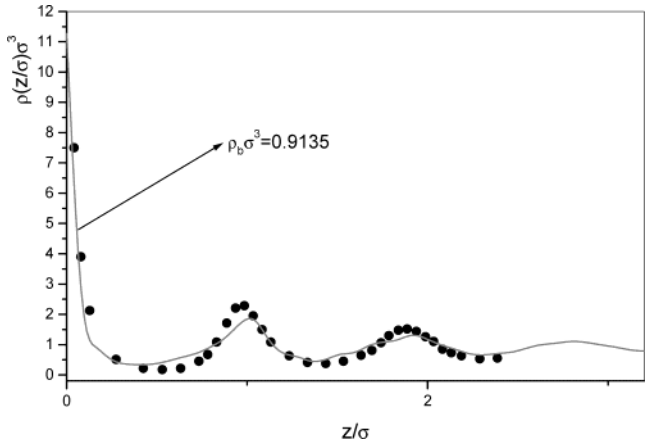

Figure 2. Density profiles of a hard-sphere fluid near a hard wall for the bulk density $\rho_b\sigma^3 = 0.9135$. Lines stand for present prediction; symbols for simulation data.[9a]

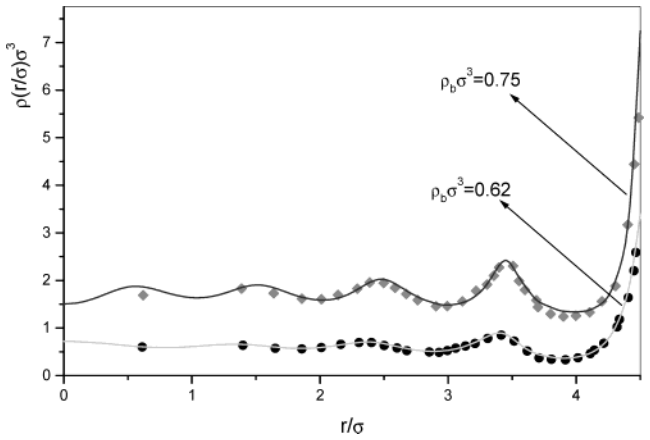

Figure 3. Density profiles of a hard-sphere fluid confined in a spherical cavity with a hard wall $R = 4.5\sigma$ for two cases of bulk density. The lines correspond to the predictions of the present method; symbols stand for the corresponding computer simulation data.[9b] The ordinate for the curve above should be shifted down 1 unit.

According to definition of the $C^{(1)}(\mathbf{r};[\rho])$,

$$C^{(1)}(\mathbf{r};[\rho]) = \frac{-\beta\delta F_{ex}[\rho]}{\delta\rho(\mathbf{r})} \quad (14)$$

By functional integration one can obtain the expression for the

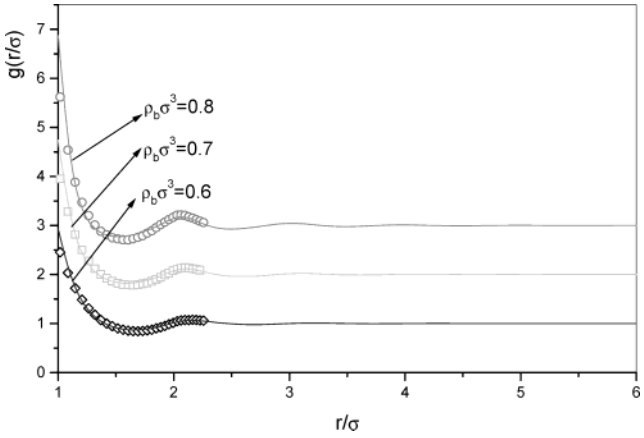

Figure 4. Comparison of the radial distribution function of the bulk hard-sphere fluid from the present DFT with the Monte Carlo simulation data[9c] for several bulk densities. The ordinate for the curve for $\rho_b = 0.8$ should be shifted down 2 units, whereas that for $\rho_b = 0.7$ should be shifted down 1 unit.

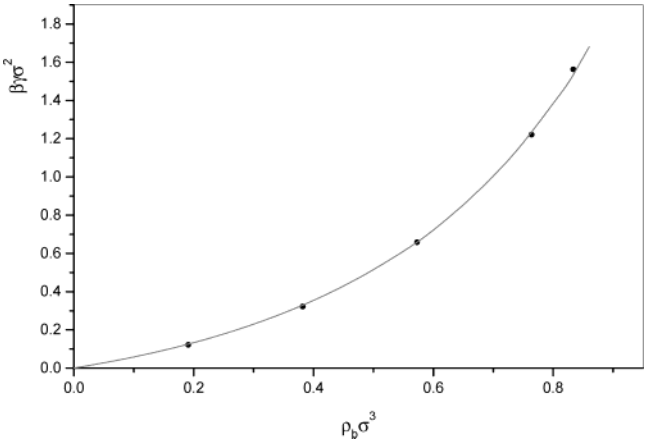

Figure 5. Surface tension $\beta\gamma\sigma^2$ of a hard-wall−hard-sphere interface as a function of the bulk hard-sphere fluid density $\rho_b\sigma^3$. The line denotes the present prediction; symbols denote the simulation data.[11]

excess Helmholtz free energy $\beta F_{ex}[\rho]$.

$$\beta F_{ex}[\rho] = -\int_0^1 d\alpha \int d\mathbf{r}\, \rho(\mathbf{r}) C^{(1)}(\mathbf{r};[\alpha\rho]) \qquad (15)$$

Here, $C^{(1)}(\mathbf{r};[\alpha\rho])$ can be calculated using eq 7 by replacing $\rho(\mathbf{r})$ and ρ_b appearing in eqs 4, 6, and 7 by $\alpha\rho(\mathbf{r})$ and $\alpha\rho_b$.

To test the validity of the present approximation, eq 7, for prediction of the global thermodynamic property $\beta F_{ex}[\rho]$, we now calculate the surface tension $\beta\gamma$ of a hard-wall−hard-sphere interface.

The grand potential Ω of a system in contact with a wall

$$\Omega = \Omega_{bulk} + \Omega_{surf} \qquad (16)$$

decomposes into a bulk contribution $\Omega_{bulk} = -pV$, given by the bulk pressure p in the system times the volume V occupied by fluid particles and a surface term $\Omega_{surf} = \gamma A$, which is the surface tension γ times the surface area A of the wall.

The grand potential Ω of a system in contact with a hard wall is

$$\Omega[\rho] = F[\rho] - \mu \int d\mathbf{r}'\, \rho(\mathbf{r}') \qquad (17)$$

Functional $F[\rho]$ decomposes into an ideal gas contribution $\beta F_{id}[\rho] = \int d\mathbf{r}'\, \rho(\mathbf{r}')[\ln(\lambda^3\rho(\mathbf{r}')) - 1]$ with λ the thermal wavelength and an excess contribution $\beta F_{ex}[\rho]$ given by eq 15. The chemical potential μ in eq 17 decomposes into a ideal gas contribution $\mu_{id} = \ln(\lambda^3\rho_b)$ and an excess contribution $\mu_{ex} = -C_0^{(1)}(\rho_b)$.

Following the above argument, one arrives at

$$\beta\gamma = \frac{\beta pV + \beta\Omega}{A} = \int_{0.5\sigma}^{H\sigma} dz\, \rho(z)\left[\ln\left(\frac{\rho(z)}{\rho_b}\right) - 1\right] + \beta pH\sigma + C_0^{(1)}(\rho_b)\int_{0.5\sigma}^{H\sigma} dz\, \rho(z) - \int_0^1 d\alpha \int_{0.5\sigma}^{H\sigma} dz\, C^{(1)}(z;[\alpha\rho])\rho(z) \qquad (18)$$

In eq 18 H should be chosen to be a large value, for example, 13, so that increasing the value of H furthermore does not change the calculated $\beta\gamma$. It should be noted that we employ the Percus−Yevick compressibility equation of state in eq 18 to ensure that, when H is increased furthermore to where the density distribution $\rho(\mathbf{r})$ reduces completely to ρ_b, the calculated $\beta\gamma$ does not change at all. The analysis is as follows.

Assuming $H\sigma$ is so large that at the region from $H\sigma$ to $H\sigma + \Delta H\sigma$, $\rho(\mathbf{r})$ completely reduces to ρ_b, we calculate the increase $\Delta\beta\gamma$ due to increasing the integral upper limit from $H\sigma$ to $H\sigma + \Delta H\sigma$ in eq 18.

$$\begin{aligned}\Delta\beta\gamma &= -\rho_b\Delta H\sigma + Z\Delta H\sigma\rho_b + \Delta H\sigma\rho_b C_0^{(1)}(\rho_b) - \int_0^1 d\alpha \int_{H\sigma}^{H\sigma+\Delta H\sigma} dz C_0^{(1)}(\alpha\rho_b)\rho_b \\ &= \rho_b\Delta H\sigma(Z-1) - \Delta H\sigma\rho_b\beta\mu_{ex}(\rho_b) + \Delta H\sigma\rho_b\beta f_{ex}(\rho_b) \qquad (19) \\ &= \Delta H\sigma\rho_b[Z - 1 - \beta\mu_{ex}(\rho_b) + \beta f_{ex}(\rho_b)]\end{aligned}$$

In eq 19, $Z - 1 - \beta\mu_{ex}(\rho_b) + \beta f_{ex}(\rho_b)$ is exactly zero only if Z, $\beta\mu_{ex}(\rho_b)$, and $\beta f_{ex}(\rho_b)$ are self-consistent, so, in order to make $\Delta\beta\gamma$ exactly zero, Z should be chosen as the Percus−Yevick compressibility equation of state since the Percus−Yevick approximation for DCFs are employed in eq 18.[8]

The calculated $\beta\gamma$ from the present approximation for $C^{(1)}(\mathbf{r};[\rho])$ denoted by eq 7 was plotted as a function of bulk density ρ_b in Figure 5 with the corresponding computer simulation data.[11] It was found that the agreement with the accurate simulation data is very good for this global thermodynamic quantity.

Now we will apply the present density functional approximation eq 7 to a nonuniform Lennard-Jones fluid. Contrary to the often-adopted procedure which divides the interaction potential itself and then treats the separated parts individually, we think that the two separated parts couple with each other; it is not reasonable to treat them individually without consideration of the coupling. However the coupling between the short-range, repulsive part and the smoothly varying, long-range, attractive tail can be taken into account by solving the Ornstein−Zernike (OZ) integral equation for the bulk second-order DCF $C_0^{(2)}(|\mathbf{r} - \mathbf{r}'|;\rho_b\cdots)$ (here $\cdots$ denotes the bulk parameters rather than the bulk density ρ_b). Because the excess Helmholtz free energy density functional $F_{ex}[\rho]$ is additive, from the definition of the DCFs

$$C^{(n)}(\mathbf{r}_1,\mathbf{r}_2,\cdots,\mathbf{r}_n;[\rho]) = \frac{-\beta\delta^n F_{ex}[\rho]}{\delta\rho(\mathbf{r}_1)\delta\rho(\mathbf{r}_2)\cdots\delta\rho(\mathbf{r}_n)} \qquad (20)$$

the DCFs of all orders are also additive. If one separates the DCF into a short-range part and a long-range tail, because the DCF has incorporated all of the nonlinear functional coupling connection between the short-range, repulsive part and the smoothly varying, long-range, attractive tail into itself, such

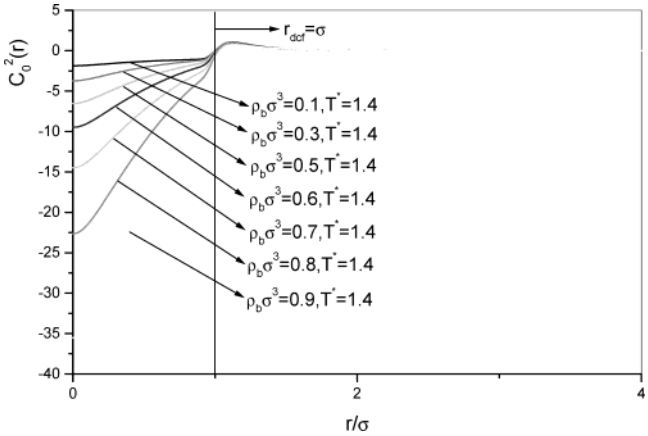

Figure 6. Bulk second-order DCF $C_0^{(2)}(r;\rho_b,T^*\cdots)$ for several bulk densities at reduced temperature $T^* = 1.35$ for the LJ potential truncated at $r_c^* = r_c/\sigma = 4$.

separation has considered the nonlinear functional dependency of the DCF on the interaction potential and the coupling between the two parts of the interaction potential.

From Figure 6 one can see that the bulk second-order DCF $C_0^{(2)}(r;\rho_b,T^*\cdots)$ is almost independent of the bulk density argument for a separation distance larger than $r_{dcf} = \sigma$. So, we divide the $C_0^{(2)}(r;\rho_b,T^*\cdots)$ into two parts, $C_{0S}^{(2)}(r;\rho_b,T^*\cdots)$ and $C_{0L}^{(2)}(r;\rho_b,T^*\cdots)$.

$$C_0^{(2)}(r;\rho_b,T^*\cdots) = C_{0S}^{(2)}(r;\rho_b,T^*\cdots) + C_{0L}^{(2)}(r;\rho_b,T^*\cdots) \quad (21)$$

here

$$C_{0S}^{(2)}(r;\rho_b,T^*\cdots) = C_0^{(2)}(r;\rho_b,T^*\cdots) \qquad r \le \sigma$$
$$= 0 \qquad r > \sigma \quad (22)$$

and

$$C_{0L}^{(2)}(r;\rho_b,T^*\cdots) = 0 \qquad r \le \sigma$$
$$= C_0^{(2)}(r;\rho_b,T^*\cdots) \qquad r > \sigma \quad (23)$$

The short-range part $C_{0S}^{(2)}(r;\rho_b,T^*\cdots)$ will be treated by the present density functional approximation eq 7, that is, $C_0^{(2)}(r;\rho_b)$, $C_0^{(1)'}(\rho_b)$, and $C_0^{(1)}(\rho_b)$ in eqs 6 and 7 will be substituted by $C_{0S}^{(2)}(r;\rho_b,T^*\cdots)$, $C_{0S}^{(1)'}(\rho_b,T^*\cdots)$, and $C_{0S}^{(1)}(\rho_b,T^*\cdots)$ here.

$$C_{0S}^{(1)'}(\rho_b,T^*\cdots) = \int d\mathbf{r}\, C_{0S}^{(2)}(\mathbf{r};\rho_b,T^*\cdots) \quad (24)$$

$$C_{0S}^{(1)}(\rho_b,T^*\cdots) = \int_0^{\rho_b}\int d\mathbf{r}\, C_{0S}^{(2)}(\mathbf{r};\rho^0,T^*\cdots)\, d\rho^0 \quad (25)$$

For the long-range part $C_{0L}^{(2)}(r;\rho_b,T^*\cdots)$ it is easy to show that if $C_{0L}^{(2)}(r;\rho_b,T^*\cdots)$ is not dependent on the bulk density ρ_b, then the following lowest order functional perturbation expansion approximation is exact.

$$C_L^{(1)}(\mathbf{r};[\rho],T^*\cdots) = C_{0L}^{(1)}(\rho_b,T^*\cdots) + \int C_{0L}^{(2)}(|\mathbf{r}-\mathbf{r}'|;\rho_b,T^*\cdots)[\rho(\mathbf{r}')-\rho_b]\, d\mathbf{r}' \quad (26)$$

If $C_{0L}^{(2)}(r;\rho_b,T^*\cdots)$ is not completely independent of the bulk density, then the more independent the $C_{0L}^{(2)}(r;\rho_b,T^*\cdots)$ is of the bulk density, the more accurate eq 26 is.

We give a simple proof of the argument as follows.

Carrying out a functional integration on the definition of the nonuniform second-order DCF with the integration path chosen as $\rho_b + \alpha(\rho - \rho_b)$

$$C_L^{(2)}(\mathbf{r},\mathbf{r}';[\rho],T^*\cdots) = \frac{\delta C_L^{(1)}(\mathbf{r};[\rho],T^*\cdots)}{\delta\rho(\mathbf{r}')} \quad (27)$$

one obtains

$$C_L^{(1)}(\mathbf{r};[\rho],T^*\cdots) = C_{0L}^{(1)}(\rho_b,T^*\cdots) + \int_0^1 d\alpha \int d\mathbf{r}'\, C_L^{(2)}(\mathbf{r},\mathbf{r}';[\rho_b+\alpha(\rho-\rho_b)],T^*\cdots)[\rho(\mathbf{r}')-\rho_b] \quad (28)$$

According to the spirit of the weighted density approximation, $C_L^{(2)}(\mathbf{r},\mathbf{r}';[\rho_b + \alpha(\rho - \rho_b)],T^*\cdots)$ can be approximated by $C_{0L}^{(2)}(|\mathbf{r} - \mathbf{r}'|;\tilde{\rho}(\mathbf{r},\mathbf{r}';\alpha),T^*\cdots)$; obviously, if $C_{0L}^{(2)}(r;\rho_b,T^*\cdots)$ is completely independent of the bulk density, then $C_L^{(2)}(\mathbf{r},\mathbf{r}';[\rho_b + \alpha(\rho - \rho_b)],T^*\cdots)$ is exactly equal to $C_{0L}^{(2)}(r;\rho_b,T^*\cdots)$. Then eq 28 reduces to eq 26.

Substituting the approximation eq 7 applied to $C_{0S}^{(2)}(r;\rho_b,T^*\cdots)$ and the approximation eq 26 for $C_{0L}^{(2)}(r;\rho_b,T^*\cdots)$ into the density profile eq 8, one can obtain

$$\rho(\mathbf{r}) = \rho_b \exp\{-\beta\varphi_{ext}(\mathbf{r}) + C_{0S}^{(1)}(\tilde{\rho}(\mathbf{r},\lambda),T^*\cdots) + \int C_{0S}^{(1)'}(\tilde{\rho}(\mathbf{r}',\lambda),T^*\cdots)\lambda w(|\mathbf{r}-\mathbf{r}'|;\rho_b)[\rho(\mathbf{r}')-\rho_b]\, d\mathbf{r} - C_{0S}^{(1)}(\rho_b,T^*\cdots) + \int d\mathbf{r}'\, C_{0L}^{(2)}(|\mathbf{r}-\mathbf{r}'|;\rho_b,T^*\cdots)[\rho(\mathbf{r}')-\rho_b]\} \quad (29)$$

The bulk second-order DCF $C_0^{(2)}(r;\rho_b,T^*\cdots)$ for a Lennard-Jones fluid is obtained by solving the OZ equation with the VM closure combined with the so-called renormalization of the indirect correlation function.[12] The interaction potential for the Lennard-Jones system is of the following form:

$$u_{LJ}(r) = 4\epsilon\left[\left(\frac{r}{\sigma}\right)^{-12} - \left(\frac{r}{\sigma}\right)^{-6}\right] \quad (30)$$

Here, σ is the interaction range parameter and ϵ is the interaction strength parameter; it is related to the reduced temperature T^* by $T^* = \{1/\beta\epsilon\}$.

The truncated LJ interaction potential is of the following form:

$$u_{LJ}^C(r) = u_{LJ}(r) \qquad r \le r_c$$
$$= 0 \qquad r \ge r_c \quad (31)$$

We study the density distribution of the Lennard-Jones fluid under an external potential denoted by eqs 10 and 11, respectively. We have performed computations with external potential eq 10 at several bulk densities for reduced temperature $T^* = 1.35$ to compare with the Monte Carlo (MC) simulation result of Balabanic et al.[13] The LJ potential is truncated at $r_c = 4.0\sigma$. The value of the cutoff distance r_c used in the MC simulations varied with bulk densities, but these values are estimated to be close to 4.0σ. The results are plotted in Figures 7−9 which show that the present approximation is significantly superior to the previous density functional mean field theory (DFMFT)[3a] result at supercritical temperature $T^* = 1.35$; compared with the previous density functional perturbation theory (DFPT),[3a] the present approximation is also superior to the former except for the region near the wall. Even if the present approximation cannot predict accurately the contact

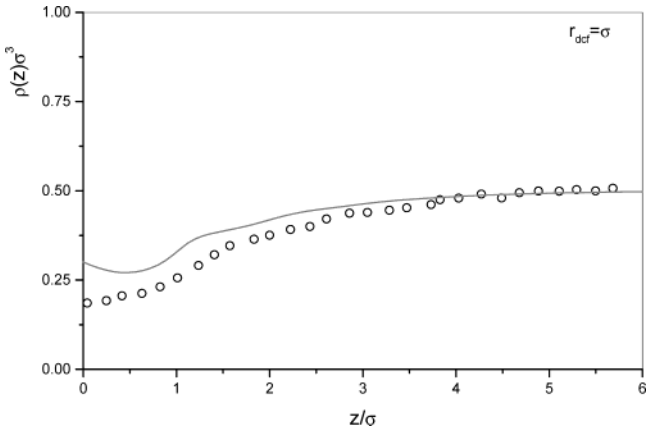

Figure 7. Density distribution profile for a LJ fluid in contact with a hard wall at the reduced temperature $T^* = 1.35$ and bulk density $\rho_b\sigma^3 = 0.5$ for the LJ potential truncated at $r_c^* = r_c/\sigma = 4$. The symbols are for the MC data;[13] the lines are for the theoretical predictions.

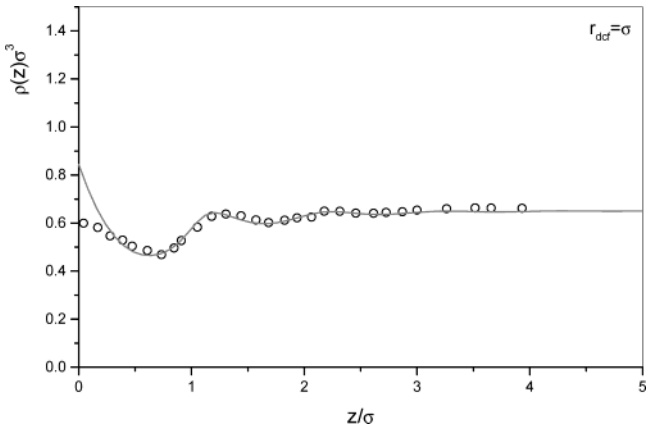

Figure 8. Density distribution profile for a LJ fluid in contact with a hard wall at the reduced temperature $T^* = 1.35$ and bulk density $\rho_b\sigma^3 = 0.65$ for the LJ potential truncated at $r_c^* = r_c/\sigma = 4$. The symbols are for the MC data;[13] the lines are for the theoretical predictions.

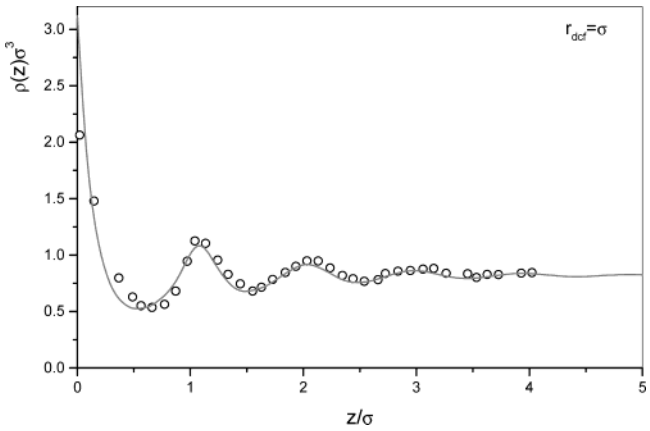

Figure 9. Density distribution profile for a LJ fluid in contact with a hard wall at the reduced temperature $T^* = 1.35$ and bulk density $\rho_b\sigma^3 = 0.82$ for the LJ potential truncated at $r_c^* = r_c/\sigma = 4$. The symbols are for the MC data;[13] the lines are for the theoretical predictions.

density, it can describe the formation of the vapor layer at the interface at the low-density region. For the case of external potential denoted by eq 11, we calculate the density distribution profile for the case of reduced temperatures $T^* = 2.719$ and $T^* = 1.953$; to compare with the simulation data,[9b] the total

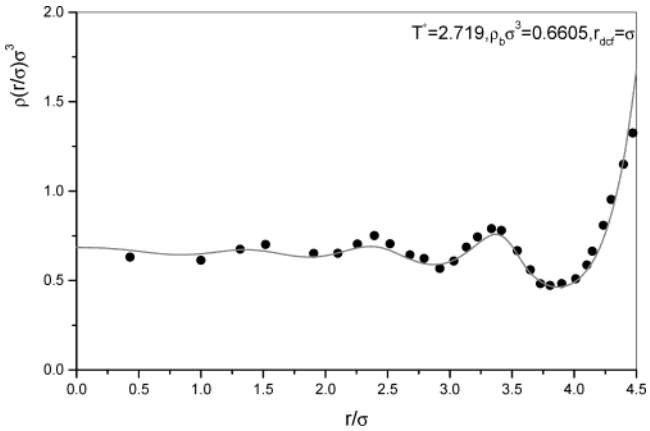

Figure 10. Density profiles of a Lennard-Jones fluid confined in a spherical cavity at the reduced temperature $\{kT\}/\{\epsilon = 2.719\}$. The dots represent the MC results;[9b] the line represents the present prediction.

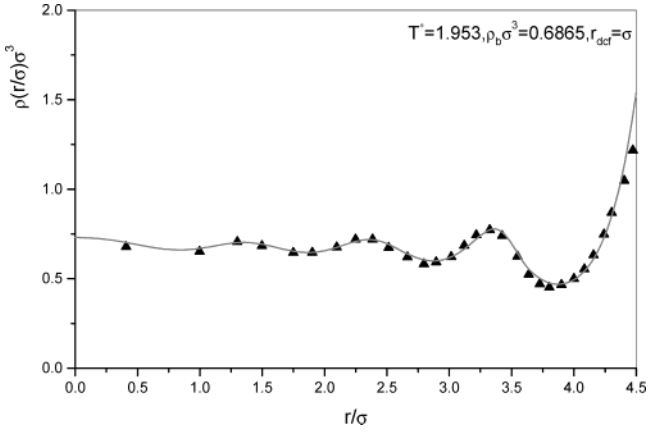

Figure 11. Density profiles of a Lennard-Jones fluid confined in a spherical cavity at the reduced temperature $\{kT\}/\{\epsilon = 1.953\}$. The dots represent the MC results;[9b] the line represents the present prediction.

particle number N in the cage

$$N = 4\pi\int_0^{R\sigma} \mathrm{d}r\ \rho(r)r^2 \tag{32}$$

is kept as a constant, $N = 266$. The calculation results are plotted in Figures 10 and 11 which display the same tendency as shown in Figures 7−9; that is, except for the contact region, the present approximation is even superior to the complicated DFPT method in ref 3b. We did not perform calculations for the reduced temperature $T^* = 1.19$, because the OZ equation cannot be solved in the whole density range from zero to the high bulk density for this reduced temperature. The reason the present approximation is not accurate at the contact region is perhaps due to the inaccuracy incurred by the approximation eq 7. However, the higher accuracy achieved by the present approximation in the region away from the contact region is obviously due to the new separation based on the bulk second-order DCF; such separation takes into account the coupling between the short-range part and long-range part of the interaction successfully.

IV. Summary

To conclude, the present paper proposes a density functional approximation for the nonuniform excess Helmholtz free energy

density functional $F_{ex}[\rho]$ and the nonuniform first-order DCF $C^{(1)}(\mathbf{r};[\rho])$; it is based on the truncated functional expansion of the $F_{ex}[\rho]$ around the bulk density, and the Lagrangian theorem of differential calculus was employed to make the truncation formally exact. To proceed numerically, the decoupled weighted density approximation was employed to approximate the $C^{(1)}(\mathbf{r};[\rho])$; then the functional derivative of the obtained nonuniform $F_{ex}[\rho]$ with respect to the density distribution leads to the new expression for $C^{(1)}(\mathbf{r};[\rho])$ whose accuracy is comparable to the previous coupled weighted density approximation.[10] The present approximation is free of any adjustable parameters, which makes its application largely convenient. For the nonhard-sphere interaction potential fluid, we propose a new partitioned density functional approximation for the $C^{(1)}(\mathbf{r};[\rho])$, which is based on dividing the bulk second-order DCF $C_0^{(2)}(r;\rho_b,T^*\cdots)$ instead of the interaction potential itself. The bulk second-order DCF $C_0^{(2)}(r;\rho_b,T^*\cdots)$ is divided into a strongly density-depending part and a weakly density-depending part; for the latter the lowest order functional perturbation expansion approximation is very accurate as shown in the present calculation. For the strongly density-depending part the approximation eq 7 is employed in the present calculation. The present separation based on the bulk second-order DCF $C_0^{(2)}(r;\rho_b,T^*\cdots)$ also can be applied in the solid−liquid phase transition by density functional theory in which the weakly density-depending part was treated by the lowest order functional perturbation expansion approximation for the nonuniform excess Helmholtz free energy density functional $F_{ex}[\rho]$; the strongly density-depending part can be treated by previous successful density functional approximations for hard-sphere model, for example, the weighted density approximation,[14] the fundamental measure functional,[15] the cell theory,[16] and so forth: we will carry out the detailed presentation and calculation in a separate paper.

Acknowledgment. This project was supported by the National Natural Science Foundation of China (Grant No. 20206033).

References and Notes

(1) (a) Henderson, D. *Fundamentals of Inhomogeneous Fluids*; Marcel Dekker: New York, 1992; p124. (b) Zhou, S.; Ruckenstein, E. *J. Chem. Phys.* **2000**, *112*, 8079. (c) Zhou, S. *Phys. Rev. E* **2001**, *63*, 051203. (d) Zhou, S. *Phys. Rev. E* **2001**, *63*, 061206.

(2) (a) Zhou, S. *New J. Phys.* **2002**, *4*, 36. (b) Zhou, S. *Chin. Phys. Lett.* **2002**, *19*, 1322. (c) Zhou, S. *J. Phys. Chem. B* **2002**, *106*, 7674. (d) Zhou, S. *Chem. Phys.* **2003**, *289*, 309. (e) Zhou, S. *J. Phys. Chem. B* **2003**, *107*, 3585. (f) Zhou, S. *Phys. Lett. A* **2003**, *319*, 279. (g) Zhou, S. *Chem. Phys.* **2004**, *297*, 171.

(3) (a) Tang, Z.; Scriven, L. E.; Davis, H. T. *J. Chem. Phys.* **1991**, *95*, 2659. (b) Kim, S.-C.; Suh, S.-H. *J. Chem. Phys.* **1996**, *104*, 7233.

(4) (a) Volterra, V. *Theory of Functionals*; Dover Publications: New York, 1959; p 26. (b) *Density-Functional Theory of Atoms and Molecules*; Parr, R. G., Yang, W., Eds.; Oxford University Press: New York; Clarendon Press: Oxford, 1989; p 249.

(5) Denton, A. R.; Ashcroft, N. W. *Phys. Rev. A* **1991**, *44*, 1219.

(6) Zhou, S. *J. Chem. Phys.* **1999**, *110*, 2140.

(7) Percus, J. K. In T*he Equilibrium Theory of Classical Fluids*, Frisch, H. L., Lebowitz, A. L., Eds,; Benjamin: New York, 1964; p 113.

(8) (a) Thiele, E. *J. Chem. Phys.* **1963**, *39*, 474. (b) Wertheim, M. S. *Phys. Rev. Lett.* **1963**, *19*, 321.

(9) (a) Groot, R. D.; Faber, N. M.; Van der Eerden, J. P. *Mol. Phys.* **1987**, *62*, 861. (b) Calleja, M.; North, A. N.; Powels, J. G.; Rickayzen, G. *Mol. Phys.* **1991**, *73*, 973. (c) Barker, J. A.; Henderson, D. *Mol. Phys.* **1971**, *21*, 187.

(10) (a) Curtin, W.A.; Ashcroft, N. W. *Phys. Rev. A* **1985**, *32*, 2909. (b) Meister, T. F.; Kroll, D. M. *Phys. Rev. A* **1985**, *31*, 4055. (c) Groot, R. D.; Eerden, v.-d. *Phys. Rev. A* **1987**, *36*, 4356.

(11) Heni, M.; Löwen, H. *Phys. Rev. E* **1999**, *60*, 7057.

(12) Choudhury, N.; Ghosh, S. K. *J. Chem. Phys.* **2002**, *116*, 8517.

(13) Balabanic, C.; Borstnik, B.; Milcic, R.; Rubcic, A.; Sokolic, F. In *Static and Dynamic Properties of Liquids*; Davidovic, M., Soper, A. K., Eds.; Springer Proceedings in Physics Vol. 40; Springer: Berlin, 1989; p 70.

(14) (a) Tarazona, P. *Mol. Phys.* **1984**, *52*, 81. (b) Tarazona, P. *Phys. Rev. A* **1985**, *31*, 2672.

(15) Tarazona, P. *Phys. Rev. Lett.* **2000**, *84*, 694.

(16) Vega, C.; Bresme, F.; Abascal, J. L. F. *Phys. Rev. E* **1996**, *54*, 2746.